J Eng Math (2015) 94:43–61
DOI 10.1007/s10665-014-9698-1

Gradient flow perspective on thin-film bilayer flows

R. Huth · S. Jachalski · G. Kitavtsev · D. Peschka

Received: 24 June 2013 / Accepted: 13 March 2014 / Published online: 30 August 2014

Abstract We study gradient flow formulations of thin-film bilayer flows with triple-junctions between liquid/liquid/air phase. First we highlight the gradient structure in the Stokes free-boundary flow and identify its solutions with the well-known PDE with boundary conditions. Next we propose a similar gradient formulation for the corresponding reduced thin-film model and formally identify solutions with those of a PDE problem. A robust numerical algorithm for the thin-film gradient flow structure is then provided. Using this algorithm we compare the sharp triple-junction model with precursor models. For their stationary solutions a rigorous connection is established using Γ-convergence. For time-dependent solutions the comparison of numerical solutions shows a good agreement for small and moderate times. Finally we study spreading in the zero-contact angle case, where we compare numerical solutions with asymptotically exact source-type solutions.

Keywords Bilayer · Contact line · Gradient flow · Thin-film

1 Introduction to liquid–liquid thin film flows

Dewetting of thin films from a solid substrate is an intensively studied subject, both from theoretical and from experimental point of view, e.g. [1] and references therein. There is known to be an intriguing interplay between the flow and the boundary condition on the substrate. For a no-slip boundary condition at the solid interface a logarithmic singularity in the dissipation prevents the triple-junction from moving and no dewetting takes place [2,3]. Due to the different nature of liquid substrates no such effects have been observed or are expected for liquid substrates. There is the fitting citation from the *Capillarity and wetting phenomena* book by de Gennes et al. [4, p. 169] explaining why liquid substrates might be just perfect to study moving contact lines:

> *Liquid substrate, smooth and homogeneous, are the epitome of perfection. However, they deform and flow. The challenge is to take into account the flows induced by the motion of the ridge.*

R. Huth · S. Jachalski · D. Peschka (✉)
Weierstrass Institute, Berlin, Germany
e-mail: peschka@wias-berlin.de

G. Kitavtsev
Max-Planck-Institute for Mathematics in the Sciences, Leipzig, Germany

Besides the classical works on liquid/liquid spreading and dewetting by Joanny [5] and Brochard-Wyart et al. [6], there are a number of works dealing with liquid substrates from a PDE perspective by using thin-film equations: Kriegsmann and Miksis [7] investigate the quasi-stationary motion of 2D-droplets on inclined substrates with gravity and sharp triple-junctions. Pototsky et al. wrote a series of papers, e.g. [8], where they investigate different possible stationary solutions of two-layer systems. Following the classical theory they compute multiple Hamaker constants which contribute to the van-der-Waals type precursor energy depending on the thickness of the different layers. In [9] Craster and Matar studied the approach of droplets toward equilibrium and equilibrium shapes of droplets. They also used a precursor layer to account for the motion of the triple-junction. In a later paper Karapetsas et al. [10] study the motion of droplets with surfactants on a liquid substrate with sharp triple-junctions. Thin-film approximations for bilayer flows were initially derived by Danov and co-workers [11] and with sharp triple-junctions by Kriegsmann [12]. Existence of weak solutions was established in [13,14].

The goal of this paper is to reconsider bilayer flows where triple-junctions are treated explicitly using a formal variational approach. Such an approach is advantageous because boundary conditions can be enforced in a rather natural and physical way and it works in any number of spatial dimensions. We also connect this approach to the more popular model with precursor.

In the remainder of this section we state thin-film models for two-layer flows as they are known in the literature. In Sect. 2 we first state a gradient formulation of the Stokes equation to motivate that such a formulation exists and how in such a case the space of solutions should be interpreted. Next we make a thin-film approximation of the driving energy. Furthermore we propose a dissipation function for the thin-film flow, identify the gradient and compare with the model formulation of [7]. Then in Sect. 3 we show that this formulation is well-suited for the construction of a robust numerical algorithm. We give a detailed explanation of the spatial and temporal discretization. A slightly non-standard trick is that we first compute time-derivatives in Eulerian coordinates and later separate them into a convective derivative and a transport of the domain which are time-derivatives in Lagrangian coordinates. Finally, in Sect. 4 we compare this approach to precursor models and asymptotic source-type solutions. As a motivation why such a comparison makes sense we make rigorous statements about convergence of stationary solutions of the precursor model as the precursor thickness tends to zero. Then we use the constructed numerical algorithm to compare dynamical solutions of the gradient model with explicit triple-junction with the precursor model. For large times and zero contact angle we derive source-type solutions and compare them with our numerical simulations.

1.1 Thin-film equations for bilayer flows

In this section we present lubrication models for liquid films on a liquid substrate. The major difference in the following models is the treatment of the triple-junction between the liquid film, the liquid substrate and the gas phase. The first approach is to incorporate an intermolecular potential which prevents that the film dewets completely. There will always remain a layer with height $h_* \ll 1$ which is called precursor. The second approach is to treat the triple-junction as a singular point (2D)/line (3D) and derive corresponding boundary conditions.

Thin-film model with precursor

A complete derivation of the model presented below can be found in [11]. Let us assume an arbitrary but fixed domain $\omega \subset \mathbb{R}^{d-1}$. In this domain we define $h_1(t,x), h(t,x)$ for time $t > 0$ to be the thickness of the liquid substrate and the liquid film at $x \in \omega$ as illustrated in Figs. 1 and 2. These height profiles are solutions of a coupled system of degenerate fourth order parabolic equations

$$\partial_t h_1 = \nabla \cdot (Q_{11}\nabla\pi_1 + Q_{12}\nabla\pi_2), \tag{1a}$$

$$\partial_t h = \nabla \cdot (Q_{21}\nabla\pi_1 + Q_{22}\nabla\pi_2), \tag{1b}$$

with mobility matrix

$$Q_{ij} = \frac{1}{\mu}\begin{pmatrix} \frac{1}{3}h_1^3 & \frac{1}{2}h_1^2 h \\ \frac{1}{2}h_1^2 h & \frac{\mu}{3}h^3 + h_1 h^2 \end{pmatrix}, \tag{1c}$$

and generalized pressures

$$\pi_1 = -(\sigma_1 + \sigma_2)\Delta h_1 - \sigma_2 \Delta h, \tag{1d}$$

$$\pi_2 = -\sigma_2 \Delta h_1 - \sigma_2 \Delta h + V_*'(h), \tag{1e}$$

where $\Delta = \nabla^2$ is the standard Laplacian. The constant μ denotes the viscosity-ratio between liquid substrate and the liquid film, while σ_1 is the surface tension at the liquid–liquid interface and σ_2 the one at the liquid–gas interface. As mentioned above this model contains the derivative of an intermolecular potential which is given by

$$V_*(h) = \frac{h_*^8}{8h^8} - \frac{h_*^2}{2h^2} + 1. \tag{1f}$$

Models of this type are very popular in this field, e.g. [9,15]. The reason is that due to the intermolecular potential one can usually avoid dealing with the degeneracy of the equation as $h \to 0$. Secondly, this approach has the advantage that it allows for quasi-topological transitions, in the sense that we have the transition from a wet substrate $h = O(1)$ to a dry substrate $h = O(h_*)$. A disadvantage of such models is that for $h_* \to 0$ second and higher order derivatives become unbounded and therefore require robust spatial and temporal adaptivity. To emphasize the dependence on the parameter h_* we will henceforth write h_1^*, h^* and refer to the model as the *precursor model*. Note that thin-film models with precursors also have an energetic structure, which in the context of two-layer models has been discussed in [8] by Thiele et al.

Thin-film model with triple-junction

Here, we recall a model derived by Kriegsmann and Miksis [7]. This model does not contain intermolecular potentials and therefore the thickness of the liquid film h can be identically zero in some parts of ω. For simplicity assume that $d = 2$, and $\omega = (0, L)$. Furthermore we assume that the region where h is positive at time t is an interval $(x_-(t), x_+(t)) \in \omega$ with $0 < x_- < x_+ < L$. In general h may be positive in different non-connected subsets of ω. For the further presentation we therefore define

$$\omega_1(t) = \big(0, x_-(t)\big), \quad \omega_2(t) = \big(x_-(t), x_+(t)\big), \quad \omega_3(t) = \big(x_+(t), L\big).$$

Now the function $h(t, x)$ is defined for $x \in \omega_2$ and $h_1(t, x)$ is defined for $x \in \omega$ and $t \geq 0$. In contrast to the thin-film equation with precursor we have a single parabolic equation on

$$\partial_t h_1 = -\partial_x \left(\frac{\sigma_1 + \sigma_2}{3\mu} h_1^3 \partial_x^3 h_1\right), \tag{2a}$$

and for $x \in \omega_1(t) \cup \omega_3(t)$ coupled to the equations

$$\partial_t h_1 = \nabla \cdot (Q_{11} \nabla \pi_1 + Q_{12} \nabla \pi_2), \tag{2b}$$

$$\partial_t h = \nabla \cdot (Q_{21} \nabla \pi_1 + Q_{22} \nabla \pi_2), \tag{2c}$$

for $x \in \omega_2(t)$. Instead of the previous π_1, π_2 we now have

$$\pi_1 = -(\sigma_1 + \sigma_2)\partial_x^2 h_1 - \sigma_2 \partial_x^2 h, \tag{2d}$$

$$\pi_2 = -\sigma_2 \partial_x^2 h_1 - \sigma_2 \partial_x^2 h. \tag{2e}$$

The constant μ still denotes the viscosity ratio while σ_1 is the surface tension at the liquid–liquid interface and σ_2 the one at the liquid–gas interface in region ω_2. In contrast to the precursor model we have an interior boundary at x_-, x_+ the so-called triple-junction. Since the three equations are of fourth order we need to equip them with six

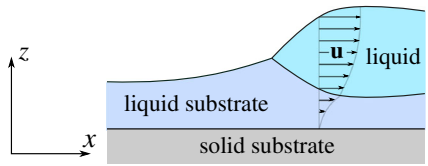

Fig. 1 Flow of a liquid on a liquid substrate above a solid substrate, where both liquids meet the ambient gaseous phase in the triple-junction

boundary conditions at x_-, x_+ each. Therefore it is useful to call $h_{1,+} = h_1\big|_{\omega_2}$ and $h_{1,0} = h_1\big|_{\omega_1 \cup \omega_3}$. Then the first two conditions address the continuity of the profiles

$$h_{1,+} - h_{1,0} = 0, \quad h = 0 \quad \text{at } x = x_\pm. \tag{2f}$$

Next, we impose the contact angles at $x_\pm$ by

$$\partial_x h_{1,+} - \partial_x h_{1,0} = -\sqrt{\frac{2\sigma\sigma_2}{\sigma_1(\sigma_1+\sigma_2)}}, \quad \partial_x h_{1,+} - \partial_x h_{1,0} + \partial_x h = \sqrt{\frac{2\sigma\sigma_1}{\sigma_2(\sigma_1+\sigma_2)}}. \tag{2g}$$

Here, σ is the spreading coefficient. Furthermore, we wish to ensure continuity of the pressure in the liquid substrate and the velocity at $x_\pm$,

$$\pi_1 + (\sigma_1+\sigma_2)\partial_x^2 h_{1,0} \quad = 0, \tag{2h}$$

$$\partial_x \pi_1 + (\sigma_1+\sigma_2)\partial_x^3 h_{1,0} = 0. \tag{2i}$$

Finally, we need one extra kinematic condition for the evolution of the contact point $x_\pm(t)$ itself, which is

$$\frac{\mathrm{d}}{\mathrm{d}t} x_\pm(t) = \lim_{x \to x_\pm} \left(\frac{\sigma_1+\sigma_2}{2\mu} h_{1,0}^2 \partial_x^3 h_{1,0} \right). \tag{2j}$$

The velocity can also be defined as an limit in terms of h. But there is a boundary condition which states that these limits are equal. In the remaining part of the paper we will refer to models where the triple-junction is treated explicitly as *sharp-interface models*. One aim of the next sections is to provide a suitable weak formulation for the model (2) and to compare its solutions with the ones to the precursor model (1).

2 Dynamics of viscous bilayers as gradient flows

In this section we derive gradient formulation of a Stokes free-boundary problem for liquid bilayers and we derive a gradient formulation for the corresponding thin-film approximation. Both liquids are immiscible, viscous and incompressible with a continuous velocity and a no-slip condition at the solid substrate as sketched in Fig. 1.

The flow is driven by the surface energy and the shape of the interfaces depends on time. Triple-junctions are treated using a sharp-interface model. We want to emphasize that it is useful to use the gradient flow structure of the system in order to identify all boundary conditions needed for the derived systems.

In this paper we skip the rather standard formal asymptotic reduction of the Stokes free-boundary problem to the thin-film equation, which can be found elsewhere [7,11]. The concept of gradient flow formulations in this class of models is well-known, e.g. works by Otto [16] or the recent study by Rumpf and Vantzos [17].

2.1 Variational approaches for free-boundary problems

Let us shortly summarize the formal construction of gradient dynamics or equivalently the dynamics of systems with Rayleigh dissipation functional [18,19]. In particular we want to focus on aspects of the construction in the context of the free-boundary problems considered in this study.

A free boundary problem is a partial differential equation, where the domain is part of the unknowns and depends on time $\Omega = \Omega(t)$. Such a PDE is usually written in Eulerian coordinates and the evolution of $\Omega(t)$ is fixed by defining the normal velocity of the boundary by a kinematic condition. By introducing a parametrization $\Psi_t : \Omega(0) \to \Omega(t)$ we can reformulate the PDE in Lagrangian coordinates $\Omega(0)$ and the dependence on $\Omega(t)$ is thereby replaced by a dependence on Ψ_t, i.e. Ψ_t becomes an unknown of the PDE and the domain is fixed.

For the free boundary Stokes problem presented in this paper Ψ_t is in fact the only unknown. Incompressibility is expressed as the constraint $\det(\nabla\Psi_t) = 1$ and the derived velocity $\mathbf{u} = \partial_t\Psi_t$ automatically satisfies $\nabla \cdot \mathbf{u} = 0$. On boundaries between a liquid and a solid we have no motion $\Psi_t = \mathrm{id}$ and thereby $\mathbf{u} = 0$. The set X of all such admissible transformations $\mathbf{s} \equiv \Psi$ is called the *space of states*, whereas the vector-space V of all admissible velocities $\dot{\mathbf{s}}$ is called the *space of velocities*. Notice that the space of admissible velocities depends on the actual state $\mathbf{s} \in X$. In the dimensionally reduced thin-film problem, we have $\Psi_t : \omega \to \omega$ and $h(t, x)$, $h_1(t, x)$ as the unknowns. The mapping Ψ_t is a one-to-one correspondence which maps each $\omega_j(0)$ to $\omega_j(t)$ for $j = 1, 2, 3$. As before we denote the set of admissible states $\mathbf{s} \equiv (\Psi, h, h_1)$ by X and the corresponding set of admissible velocities $\dot{\mathbf{s}} = (\dot{\Psi}, \dot{h}, \dot{h}_1)$ by V.

In order to construct the gradient dynamics assume we have a function $E : X \to \mathbb{R}$ which is called the energy and a symmetric bilinear form $D : V \times V \to \mathbb{R}$ which is called the dissipation. In our particular construction the dissipation depends on the state $\mathbf{s}$. Then $\mathrm{grad}_D E$ is the D-gradient of E and is defined as the element of V for which

$$D(\mathrm{grad}_D E(\mathbf{s}), \mathbf{u}) = \mathrm{diff}\, E(\mathbf{s})[\mathbf{u}] \tag{3a}$$

for all $\mathbf{u} \in V$. With $\mathrm{diff}\, E(\mathbf{s})[\mathbf{u}]$ we denote the conventional directional derivative of E at $\mathbf{s}$ in the direction of $\mathbf{u}$. A D-gradient flow with respect to an energy E is a curve $\mathbf{s}(t)$ in X which satisfies

$$\partial_t \mathbf{s}(t) = -\mathrm{grad}_D E\big(\mathbf{s}(t)\big). \tag{3b}$$

In the next part of the paper we show, that both the Stokes equation and the thin-film equation can be formulated as gradient flows. We will see that the obtained gradient flows directly provide a weak formulation for the corresponding systems, which is suitable for a numerical discretization.

This construction of the gradient of functionals is formally equivalent to the usual gradient of a function $E\colon \mathbb{R}^n \to \mathbb{R}$, which uses the Euclidean scalar product as a bilinear form $\langle\cdot,\cdot\rangle$ to define the gradient as $\langle \mathrm{grad}\, E(x), v\rangle = \mathrm{diff}\, E(x)[v] = \sum_i \partial_i E(x) v^i$ for all $v \in \mathbb{R}^n$.

An alternative viewpoint on the gradient construction is provided by Rayleigh's dissipation principle without kinetic energy. It describes an overdamped system, where the driving force diff E is balanced by viscous friction, where $\frac{1}{2}D$ is the well-known Rayleigh dissipation functional. There we find the solution curve $\mathbf{s}(t)$ by demanding that

$$\partial_t \mathbf{s}(t) = \operatorname*{argmin}_{\mathbf{u}\in V}\Big(\frac{1}{2}D(\mathbf{u}, \mathbf{u}) + \mathrm{diff}\, E(\mathbf{s})[\mathbf{u}]\Big), \tag{4}$$

where by formally taking the derivative with respect to $\mathbf{u}$ we get (3) again. With this little preparation we are ready to study gradient flows of the Stokes free boundary problem and the thin-film equations for viscous bilayer systems.

2.2 Stokes flow

Consider the free-surface flow of two viscous, immiscible liquids in the half-space $\Omega(t) = \Omega_1(t) \cup \Omega_2(t) \subset \omega \times \mathbb{R}^+$ where $\omega \subset \mathbb{R}^{d-1}$. The dynamics is parameterized by the *continuous* flow map Ψ_t with $\Omega_\ell(t) = \Psi_t\big(\Omega_\ell(0)\big)$ for $\ell = 1, 2$. Incompressibility implies that the velocity $\mathbf{u} := \partial_t\Psi_t$ obeys $\nabla \cdot \mathbf{u} = 0$. For fixed time assume that the domains can be parameterized by functions $h_1(t, \cdot)$, $h(t, \cdot) : \omega \to \mathbb{R}$ as follows:

$$\Omega_1(t) := \{(x, z) \in \omega \times \mathbb{R}^+ : 0 < z < h_1(t, x)\},$$
$$\Omega_2(t) := \{(x, z) \in \omega \times \mathbb{R}^+ : h_1(t, x) < z < h_1(t, x) + h(t, x)\},$$

Fig. 2 Sketch of geometry

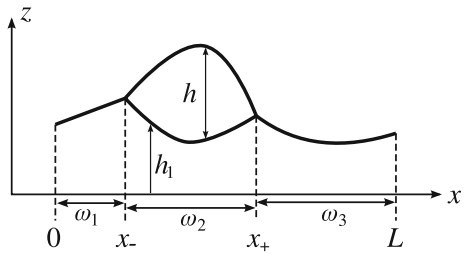

and restrict to situations where $0 < h_1 \leq h_1 + h$. For ease of notation assume that we are in $d = 2$ and have $\omega = (0, L)$. Then let $0 < x_-(t) < x_+(t) < L$ given and define as before $\omega_1(t) = \big(0, x_-\big), \omega_2(t) = \big(x_-, x_+\big), \omega_3(t) = \big(x_+, L\big)$. We have the free interfaces

$$\begin{aligned}
&\text{liquid 1–liquid 2:} && \Gamma_1(t) = \{(x,z) : x \in \omega_2, z = h_1(t,x)\}\\
&\text{liquid 2–gas:} && \Gamma_2(t) = \{(x,z) : x \in \omega_2, z = h_1(t,x) + h(t,x)\}\\
&\text{liquid 1–gas:} && \Gamma_3(t) = \{(x,z) : x \in (\omega_1 \cup \omega_3), z = h_1(t,x)\}
\end{aligned}$$

and triple-junction at $\{x, z\} = \{x_\pm(t), h_1(t, x_\pm)\}$. This constitutes a typical droplet-like configuration as it is also shown in Fig. 2. The space of states X consists of all Ψ_t which map $\Omega_1(0), \Omega_2(0)$ to $\Omega_1(t), \Omega_2(t)$ and can be written as described above.

Since early works of Rayleigh, Helmholtz and Korteweg it is known that viscous flows minimize the dissipated energy, e.g. [18,19]. For given initial domains Ω_1, Ω_2 the key ingredients to construct the Stokes free-boundary PDE formulation for $\mathbf{s} \equiv \Psi$ are the surface energy

$$E(\mathbf{s}(t)) := \sum_{j=1}^{3} \int_{\Gamma_j(t)} \gamma_j \, \mathrm{d}\Gamma, \tag{5}$$

where γ_j specifies the amount of energy carried by $\Gamma_j(t)$ per unit area. The dependence on $\mathbf{s}(t) = \Psi_t$ is due to the fact that $\Gamma_j(t) = \Psi_t(\Gamma_j(0))$. The dissipation D is defined as the energy per time to change a state with velocity $\mathbf{u}$ and for Newtonian liquids it is given by

$$D(\mathbf{u}, \mathbf{u}) = \sum_{\ell=1}^{2} \frac{\mu_\ell}{4} \int_{\Omega_\ell(t)} (\nabla \mathbf{u} + \nabla \mathbf{u}^{\mathrm{T}}) : (\nabla \mathbf{u} + \nabla \mathbf{u}^{\mathrm{T}}) \, \mathrm{d}\Omega, \tag{6}$$

where μ_ℓ are the dynamic viscosities of both liquids and the integrand is defined using the Frobenius product $A : B = \sum_{ij} A_{ij} B_{ij}$. Following the least dissipation principle, a solution of the Stokes free-boundary problem satisfies

$$\frac{\partial}{\partial t}\mathbf{s}(t) = \operatorname*{argmin}_{\mathbf{u}} \big(\tfrac{1}{2} D(\mathbf{u}, \mathbf{u}) + \operatorname{diff} E(\mathbf{s})[\mathbf{u}]\big), \tag{7}$$

which is equivalent to writing $\partial_t \Psi_t = -\operatorname{grad}_D E(\Psi_t)$. The variational principle requires the calculation of the directional derivative

$$\operatorname{diff} E(\mathbf{s})[\mathbf{v}] = -\sum_{j=1}^{3} \gamma_j \left((d-1) \int_{\Gamma_j} \kappa \mathbf{n} \cdot \mathbf{v} \, \mathrm{d}\Gamma - \mathbf{v} \cdot \mathbf{n}_{\Gamma_j} \Big|_{x_-, x_+} \right). \tag{8}$$

The vector $\mathbf{n}\kappa$ is the normal vector multiplied with the signed mean curvature of Γ_j. With $\mathbf{n}_{\Gamma_j}$ we denote the outer normal to $\partial\Gamma_j$. The necessary condition for (7) is that $D(\mathbf{u}, \mathbf{v}) = -\operatorname{diff} E(\mathbf{s})[\mathbf{v}]$ for all $\mathbf{v} \in V$. Using integration by parts in $D(\mathbf{u}, \mathbf{v})$ and $\Pi_\ell = \mu_\ell(\nabla \mathbf{u} + \nabla \mathbf{u}^\top)$ gives

$$-\sum_{\ell=1}^{2} \int_{\Omega_\ell} \big(\nabla \cdot \Pi_\ell\big) \cdot \mathbf{v} \, \mathrm{d}\Omega + \int_{\cup \Gamma_j} \mathbf{v} \cdot \big([[\Pi_\ell]] \mathbf{n} - (d-1)\gamma_j \kappa \mathbf{n} \big) \, \mathrm{d}\Gamma + \sum_j \mathbf{v} \cdot \gamma_j \mathbf{n}_{\Gamma_j} \Big|_{\{x_\pm, h(t, x_\pm)\}} = 0 \tag{9}$$

with $[[\Pi_\ell]]\mathbf{n} = (\Pi_2 - \Pi_1)\mathbf{n}$ denoting the jump across the interface. Since each term vanishes separately we get $\nabla \cdot \Pi_\ell = 0$ in Ω_ℓ, $[[\Pi_\ell]]\mathbf{n} = (d-1)\gamma_j \mathbf{n}$ on Γ_j, and the Neumann triangle condition [20] stating $\gamma_1 \mathbf{n}_{\Gamma_1} + \gamma_2 \mathbf{n}_{\Gamma_2} + \gamma_3 \mathbf{n}_{\Gamma_3} = 0$ at triple-junctions $\{x_\pm, h_1(t, x_\pm)\}$. This formulation is equivalent to the one used by Kriegsmann [7] as the basis for the further thin-film approximation.

In order to perform a thin-film approximation in the energy E one can rewrite

$$E(\Psi_t) \equiv E(h_1, h) = \int_\omega \sigma_1(x)\sqrt{1 + |\nabla h_1|^2} + \sigma_2(x)\sqrt{1 + |\nabla(h_1 + h)|^2}\,\mathrm{d}x,$$

where

$$\sigma_1(x) = \begin{cases} \gamma_1 & x \in \omega_2, \\ \gamma_3 - C & \text{else}, \end{cases} \qquad \sigma_2(x) = \begin{cases} \gamma_2 & x \in \omega_2, \\ C & \text{else}, \end{cases}$$

where we have introduced an arbitrary constant C since $h = 0$ on $\omega_1 \cup \omega_3$.

A small-slope approximation $[h] = \varepsilon[x]$ of E in powers of ε gives

$$E = \int_\omega \sigma_1(x) + \sigma_2(x) + \varepsilon^2 \left(\frac{\sigma_1(x)}{2} |\nabla h_1|^2 + \frac{\sigma_2(x)}{2} |\nabla(h_1 + h)|^2 \right) \mathrm{d}x + O(\varepsilon^4).$$

To balance the nontrivial leading order terms we expand $\gamma_i = \gamma_i^0 + \gamma_i^1 \varepsilon^2 + O(\varepsilon^4)$ and get $\gamma_1^0 + \gamma_2^0 - \gamma_3^0 = 0$. Then the next order is

$$\varepsilon^{-2}\big(E + o(1)\big) = F(h_1, h) := \int_\omega \frac{\sigma_1}{2} |\nabla h_1|^2 + \frac{\sigma_2}{2} |\nabla(h_{1+h})|^2 + \sigma(x)\mathrm{d}x, \tag{10}$$

where with $C = \gamma_2^0$ we get

$$\sigma_1 = \gamma_1^0, \qquad \sigma_2 = \gamma_2^0,$$

$$\sigma(x) = (-\sigma)\chi\{h > 0\} = \begin{cases} -\sigma & x \in \omega_2, \\ 0 & \text{else}, \end{cases}$$

with spreading coefficient $\sigma = \gamma_3^1 - \gamma_1^1 - \gamma_2^1$. In a dewetting scenario we have $\sigma < 0$. To leading order in ε we have that F in (10) is equivalent to E. A similar line of arguments has been used by Kriegsmann and Miksis in [7]. Now we are going to construct a thin-film gradient flow based on the energy F.

2.3 Thin-film flow

In this section we introduce a formal gradient structure for the bilayer thin-film flow. As before the domains Ω_1, Ω_2 are defined by continuous functions $h_1(t, \cdot) : \omega \to \mathbb{R}$ and $h(t, \cdot) : \omega_2(t) \to \mathbb{R}$, where $\omega_2 = \big(x_-(t), x_+(t)\big)$, $\omega = (0, L)$ and $0 < x_-(t) < x_+(t) < L$. Furthermore, the volumes

$$m_1(t) = \int_\omega h_1(t, x)\,\mathrm{d}x, \quad m_2(t) = \int_{\omega_2} h(t, x)\,\mathrm{d}x$$

are conserved, i.e. $m_1(t), m_2(t)$ are in fact constant in time. These conditions define the space of states, where an element $\mathbf{s} \in X$ is given by the triple $\mathbf{s} = (\Psi, h, h_1)$ for fixed volumes m_1, m_2.

In a purely Lagrangian coordinate system in fact we need to consider $\mathbf{s} \simeq (\Psi_t, h(t, \Psi_t(\cdot)), h_1(t, \Psi_t(\cdot))$ as the unknowns. The choice of $\mathbf{s}$ leading to h, h_1 in the Eulerian coordinate system is still not unique because Ψ_t is arbitrary inside $(0, x_-)$, (x_-, x_+) and (x_+, L) and only the conditions

$$\Psi_t(0) = 0, \quad \Psi_t(x_-(0)) = x_-(t), \quad \Psi_t(x_+(0)) = x_+(t), \quad \Psi_t(L) = L, \tag{11}$$

have to be satisfied. In one dimension we fix the ambiguity by choosing the piecewise linear continuation of Ψ_t which satisfies (11) in each of those intervals. Then Ψ_t is uniquely parametrized by the values $(x_-(t), x_+(t))$ and

therefore instead we consider the space of states X with $\mathbf{s} = \big(h_1, h, x_-, x_+\big)$ being the unknowns. Naturally this induces a space of velocities V and a solution is a curve $\mathbf{s}(t) \in X$ which is a gradient of the energy F for some yet to be determined dissipation D.

Now we specify the space of velocities. Instead of characterizing V in terms of partial derivatives of $H(t,x) = h(t, \Psi_t(x))$ and $H_1(t,x) = h_1(t, \Psi_t(x))$ with respect to time it will be useful to consider partial derivatives $\dot{h}(t,x) := \partial_t h(t,x)$ and $\dot{x}_\pm := dx_\pm/dt$ in the Eulerian system. Provided that solutions $h_1,\ h$ are sufficiently smooth in space and time, then they fulfill the following continuity conditions. The first one

$$\frac{\mathrm{d}}{\mathrm{d}t} h\big(t, x_\pm(t)\big) = 0$$

follows from $h\big(t, x_\pm(t)\big) = 0$. This implies that changes $\dot{h}$ and $\dot{x}_\pm$ are related by

$$\dot{h}(t, x_-) + \dot{x}_- \cdot \nabla h(t, x_-) = 0, \qquad \dot{h}(t, x_+) + \dot{x}_+ \cdot \nabla h(t, x_+) = 0. \tag{12a}$$

Note that the gradient ∇h is only defined inside (x_-, x_+), so this is the one-sided limit. Furthermore we have continuity of h_1 which implies

$$\lim_{\varepsilon \searrow 0} \frac{\mathrm{d}}{\mathrm{d}t} h_1\big(t, x_-(t)+\varepsilon\big) = \lim_{\varepsilon \nearrow 0} \tfrac{\mathrm{d}}{\mathrm{d}t} h_1\big(t, x_-(t)+\varepsilon\big), \qquad \lim_{\varepsilon \searrow 0} \tfrac{\mathrm{d}}{\mathrm{d}t} h_1\big(t, x_+(t)+\varepsilon\big) = \lim_{\varepsilon \nearrow 0} \tfrac{\mathrm{d}}{\mathrm{d}t} h_1\big(t, x_+(t)+\varepsilon\big),$$

which again implies

$$[[\dot{h}_1 + \dot{x}_- \cdot \nabla h_1]]_{x_-} = 0, \qquad [[\dot{h}_1 + \dot{x}_+ \cdot \nabla h_1]]_{x_+} = 0 \tag{12b}$$

with the notation $[[g]]_{x_\pm} = \lim_{x \nearrow x_\pm} g(x) - \lim_{x \searrow x_\pm} g(x)$ to express the jump of a quantity across $x_\pm$. So working with partial derivatives with respect to time in the Eulerian coordinate system, the time-derivatives $(\dot{h}_1, \dot{h}, \dot{x}_-, \dot{x}_+)$ should obey the compatibility conditions (12) to be admissible velocities. The purpose of these equation is soley to ensure continuity of the height profiles h, h_1 at $x_\pm$. We want to remark that the introduction of space of states with compatibility conditions is natural but at this point rather formal. However, these definitions are extensions of the analytical framework for the non-zero contact angle solutions of thin-film equations by Otto in [21] to thin bilayer films.

Further, we define formally the bilinear form $D_{\mathbf{s}} : V \times V \to \mathbb{R}$ as follows. First define the auxiliary pressures $\pi_1,\ \pi_2$ as weak solutions of

$$\int_\omega \dot{h}_1 \phi_1 + Q_{11} \nabla \pi_1 \cdot \nabla \phi_1 \,\mathrm{d}x + \int_{\omega_2} Q_{12} \nabla \pi_2 \cdot \nabla \phi_1 \,\mathrm{d}x = 0, \tag{13a}$$

$$\int_{\omega_2} \dot{h} \phi_2 + (Q_{21} \nabla \pi_1 + Q_{22} \nabla \pi_2) \cdot \nabla \phi_2 \,\mathrm{d}x = 0, \tag{13b}$$

for all ϕ_1, ϕ_2 considered with a symmetric matrix for $h_1, h > 0$

$$Q_{ij} = \frac{1}{\mu} \begin{pmatrix} \frac{1}{3} h_1^3 & \frac{1}{2} h_1^2 h \\ \frac{1}{2} h_1^2 h & \frac{\mu}{3} h^3 + h_1 h^2 \end{pmatrix}.$$

The definition of π_i through this weak formulation implies for the flux

$$J_i := \sum_j Q_{ij} \nabla \pi_j = 0 \quad \text{at} \quad x = \{0, L\}, \quad [[J_1]] = 0 \quad \text{and} \quad J_2 = 0 \quad \text{at } x_\pm,$$

as a natural boundary condition and basically implies conservation of volumes $\dot{m}_1 = \dot{m}_2 = 0$. As in the previous section $\mu = \mu_1/\mu_2$ is the ratio of the viscosities. Note that $\dot{h}_1$ jump at $x_\pm$ but π_1 is continuous. Both pressures π_i are only defined up to an additive constant, which we fix by requiring

$$\int_\omega \pi_1 \,\mathrm{d}x = \int_{\omega_2} \pi_2 \,\mathrm{d}x = 0. \tag{14}$$

Now, we define the bilinear form by

$$D_{\mathbf{s}}(\dot{\mathbf{s}}, \dot{\mathbf{s}}) = \sum_{i,j=1}^{2} \int Q_{ij} \nabla \pi_i \cdot \nabla \pi_j \, \mathrm{d}x, \tag{15}$$

where the term with Q_{11} is integrated over ω and the rest only over ω_2. As $\{\pi_1, \pi_2\}$ depend linearly on $\dot{\mathbf{s}} \equiv (\dot{h}_1, \dot{h}, \dot{x}_-, \dot{x}_+)$ by (13) it follows that (15) defines a symmetric bilinear form. Let us further consider the energy $F : X \to \mathbb{R}$

$$F(h_1, h) = \int_{\omega} e(x, h_1, h) \, \mathrm{d}x,$$

which we introduced earlier, where e is the abbreviation for

$$e(x, h_1, h) := \frac{\sigma_1}{2} |\nabla h_1|^2 + \frac{\sigma_2}{2} |\nabla (h_1 + h)|^2 + \sigma(x).$$

The Rayleigh principle applied to F considered with the bilinear form (15) implies that for a solution $\mathbf{s}(t)$ we have

$$\partial_t \mathbf{s} = \operatorname{argmin} \left(\frac{1}{2} D_{\mathbf{s}}(\dot{\mathbf{s}}, \dot{\mathbf{s}}) + \operatorname{diff} F(\mathbf{s})[\dot{\mathbf{s}}] \right).$$

This is equivalent to

$$D_{\mathbf{s}}(\dot{\mathbf{s}}, \dot{\tilde{\mathbf{s}}}) = -\operatorname{diff} F(\mathbf{s})[\dot{\tilde{\mathbf{s}}}]$$

for all $\dot{\tilde{\mathbf{s}}} \in V$. This is the basic weak formulation, which we will use in the next section to compute numerical solution. There we will propose a definition of a time-step in X which is compatible with its nonlinear structure.

In this section it remains to formally identify the gradient, so that we are able to compare with the well-known PDE formulation of bilayer flows. Therefore we perform integration by parts in the bilinear form

$$D_{\mathbf{s}}(\dot{\mathbf{s}}, \dot{\tilde{\mathbf{s}}}) = \int Q_{ij} \nabla \pi_j \cdot \nabla \tilde{\pi}_i \, \mathrm{d}x = \int -\nabla \cdot \left(Q_{ij} \nabla \tilde{\pi}_i \right) \pi_j \, \mathrm{d}x = \int -\left(\dot{\tilde{h}}_1 \pi_1 + \dot{\tilde{h}} \pi_2 \right) \mathrm{d}x$$

and in the derivative of the energy

$$\begin{aligned} \operatorname{diff} F(\mathbf{s})[\dot{\tilde{\mathbf{s}}}] &= \int_{\omega} \sigma_1 \nabla h_1 \cdot \nabla \dot{\tilde{h}}_1 + \sigma_2 (\nabla h_1 + \nabla h) \cdot (\nabla \dot{\tilde{h}}_1 + \nabla \dot{\tilde{h}}) \mathrm{d}x + \int_{\partial \omega_2} [[e]] \, \dot{\tilde{x}} \cdot \mathbf{n} \\ &= -\int_{\omega} \sigma_1 \Delta h_1 \dot{\tilde{h}}_1 + \sigma_2 (\Delta h_1 + \Delta h)(\dot{\tilde{h}}_1 + \dot{\tilde{h}}) \mathrm{d}x + \int_{\partial \omega_2} [[e + b]] \, \dot{\tilde{x}} + [[c]] \dot{\tilde{H}}_1. \end{aligned} \tag{16}$$

The term $b := -\sigma_1 |\nabla h_1|^2 - \sigma_2 |\nabla (h_1 + h)|^2$ comes from integration by parts using (12) and $c := \sigma_1 \nabla h_1 + \sigma_2 \nabla (h_1 + h)$. Comparing the expressions in $D_{\mathbf{s}}$ and diff F for all $\dot{\tilde{\mathbf{s}}}$ we find that the pressures π_i are

$$\pi_1 = -(\sigma_1 + \sigma_2) \Delta h_1 - \sigma_2 \Delta h, \qquad \pi_2 = -\sigma_2 (\Delta h_1 + \Delta h) \tag{17}$$

in ω and ω_2 respectively. Since $\dot{\tilde{x}}$, $\dot{\tilde{H}}_1 := \dot{\tilde{h}}_1 + \dot{\tilde{x}} \cdot \nabla h_1$ can be varied independently we get

$$[[e + b]] = 0, \quad [[c]] = 0 \quad \text{at } x = x_{\pm}. \tag{18}$$

A simple calculation shows that these conditions are equivalent to (2g). Finally, one obtains a closed PDE system for $h_1(t, x)$, $h(t, x)$ and the corresponding points $x_{\pm}(t)$

$$\dot{h}_1 - \nabla \cdot (Q_{11} \nabla \pi_1 + Q_{12} \nabla \pi_2) = 0, \qquad \dot{h} - \nabla \cdot (Q_{21} \nabla \pi_1 + Q_{22} \nabla \pi_2) = 0 \tag{19}$$

combined with (17), the boundary conditions prescribed by (18) and the conservation of volume. Note that in $\omega_1 \cup \omega_3$ we have $Q_{12} = Q_{21} = Q_{22} = 0$ and thereby

$$\dot{h}_1 + \nabla \cdot \left(\frac{(\sigma_1 + \sigma_2) h_1^3}{3\mu} \nabla \Delta h_1 \right) = 0, \quad \dot{h} = 0, \tag{20}$$

which is the standard thin-film equation for a single layer of height h_1. Thereby, the derived gradient system coincides with the PDE formulation as introduced by Kriegsmann [7].

Let us comment again on advantages of the Rayleigh dissipation formulation in comparison with the PDE formulation that was stated in the introduction. The main advantage is concerned with the six boundary condition, which need to be enforced at each $x_\pm$. Continuity of h_1 and h is directly in the definition of the space of states and implies continuity of velocities in Lagrangian coordinates. Working in Eulerian coordinates we get extra compatibility conditions (12), which one might consider as essential boundary conditions. The Neumann contact angles and continuity of the flux J_1 is satisfied due to natural boundary conditions. The pressure π_1 is continuous across $x_\pm$ by definition.

Furthermore, an underlying variational structure allows effectively for determination of the equilibrium states by minimizing energies E or F.

Finally, we explore numerically the variational structure in the next section by first discretizing the variational problem in space and time. The resulting numerical algorithm has the advantages of the method above, i.e., boundary conditions at $x_\pm$ are imposed in a natural way.

3 Numerical algorithm

Let us consider the gradient formulation as stated before in the form

$$D_{\mathbf{s}}(\dot{\tilde{\mathbf{s}}}, \dot{\mathbf{s}}) = -\operatorname{diff} F(\mathbf{s})[\dot{\tilde{\mathbf{s}}}],$$

which has to hold for all admissible velocities $\dot{\tilde{\mathbf{s}}} \in V$, i.e. a solution needs to fulfill the linear homogeneous constraints in Eqs. (12, 13, 14). Suppose that we have already discretized the problem, e.g. using P_1 finite elements. In general it might be difficult to enforce all these linear homogeneous constraints explicitly. Since our problem is equivalent to a quadratic minimization problem, it is only natural to enforce linear constraints by the method of Lagrange multipliers, i.e. we seek solutions $\dot{\mathbf{s}}$ and Lagrange multipliers λ such that

$$D_{\mathbf{s}}(\dot{\mathbf{s}}, \dot{\tilde{\mathbf{s}}}) + C(\lambda, \dot{\tilde{\mathbf{s}}}) = -\operatorname{diff} F(\mathbf{s})[\dot{\tilde{\mathbf{s}}}], \tag{21a}$$

$$C(\tilde{\lambda}, \dot{\mathbf{s}}) = 0 \tag{21b}$$

for all $\dot{\tilde{\mathbf{s}}}$ and multiplier $\tilde{\lambda}$. Please note that each constraint is accompanied by a transposed term which consistently couples the multiplier to the actual problem. The constraint C explicitly includes the discretized weak form of (13) and (14) and the point-wise evaluations of the constraints in (12). A similar approach is used by Rumpf and Vantzos [17] to enforce the conservation law as a constraint. Explicitly we use for C the following set of linear constraints

$$\begin{aligned} C(\tilde{\lambda}, \dot{\mathbf{s}}) = & \int_\omega \dot{h}_1 \tilde{\lambda}_1 + Q_{11} \nabla \pi_1 \cdot \nabla \tilde{\lambda}_1 \mathrm{d}x + \int_{\omega_2} Q_{12} \nabla \pi_2 \cdot \nabla \tilde{\lambda}_1 \, \mathrm{d}x \\ & + \int_{\omega_2} \dot{h} \tilde{\lambda}_2 + (Q_{21} \nabla \pi_1 + Q_{22} \nabla \pi_2) \cdot \nabla \tilde{\lambda}_2 \, \mathrm{d}x \\ & + \Big(\dot{h}(t, x_\pm) + \dot{x}_\pm \cdot \nabla h(t, x_\pm) \Big) \tilde{\lambda}_\pm^h + \Big([[\dot{h}_1 + \dot{x}_\pm \cdot \nabla h_1]]_{x_\pm} \Big) \tilde{\lambda}_\pm^{h_1} \\ & + \tilde{\lambda}_{\pi_1} \int_\omega \pi_1 \, \mathrm{d}x + \tilde{\lambda}_{\pi_2} \int_{\omega_2} \pi_2 \, \mathrm{d}x, \end{aligned} \tag{22}$$

where $\tilde{\lambda}_\pm^h, \tilde{\lambda}_\pm^{h_1}, \tilde{\lambda}_{\pi_1}, \tilde{\lambda}_{\pi_1} \in \mathbb{R}$ and $\tilde{\lambda}_1, \tilde{\lambda}_2$ are continuous functions from our discrete finite element space. Let us emphasize again that $\dot{h}_1$ is not continuous at $x_\pm$. Let us make some further remarks regarding the space and time

discretization. In order to discretize the gradient formulation in space we use the Galerkin method with standard piecewise linear finite elements φ_i, χ_i and represent discrete solutions by

$$\dot{h}_1(x) = \sum_i \dot{h}_1^i \varphi_i(x), \quad \dot{h}(x) = \sum_i \dot{h}^i \varphi_i(x),$$

where φ_i might jump at $x_\pm$. Since we use nodal elements we need to perform a double-counting of degrees of freedoms at $x_\pm$. Note that the coefficients $\dot{h}^i$ only multiply basis functions φ_i which are supported in ω_2. The auxiliary variable π_1 is continuous and π_2 is again only defined on ω_2, so we have

$$\pi_1(x) = \sum_i \pi_1^i \chi_i(x), \quad \pi_2(x) = \sum_i \pi_2^i \chi_i(x).$$

The test-functions $\tilde{\lambda}_1$, $\tilde{\lambda}_2$ in (22) are continuous and we use

$$\tilde{\lambda}_1(x) = \sum_i \lambda_1^i \chi_i(x), \quad \tilde{\lambda}_2(x) = \sum_i \lambda_2^i \chi_i(x).$$

All basis functions considered above are piecewise linear and only differ in their continuity properties at $x_\pm$ and on their domain of definition, i.e. they are either defined on ω or only on ω_2. Finally this leads to a discrete problem, where we seek the vectors of coefficients

$$\dot{\mathbf{s}} = (\dot{h}_1, \dot{h}, \pi_1, \pi_2, \dot{x}_-, \dot{x}_+)^{\mathrm{T}}$$

and seek Lagrange multipliers λ for the constraints in C. The multiplier has components $\lambda = (\lambda_1, \lambda_2, \lambda_\pm^h, \lambda_\pm^{h_1}, \lambda_{\pi_2}, \lambda_{\pi_2})$. For the construction of the global matrix it makes sense to distinguish coefficients for basis functions, which are supported in ω_k for $k = 1, 2, 3$. Therefore we introduce the notation $\dot{h}_{1,k}$ for $\dot{h}_1$ in ω_k and $\dot{h}_{0,2}$ for $\dot{h}$ in ω_2. The corresponding counting of degrees of freedom for a small mesh with 8 vertices is illustrated in Fig. 3. Note again that $\dot{h}_1$ is discontinuous, π_1 is continuous, and $\dot{h}$, π_2 are defined on ω_2.

Using these definitions our weak formulation $D_{\mathbf{s}}(\dot{\mathbf{s}}, \cdot) = -\mathrm{diff}\, F(\mathbf{s})$ can be written in a block-form as follows:

$$D\dot{\mathbf{s}} = \left(\begin{array}{c|cc|c} \tau(\sigma S) & & & \\ \hline & Q_{11}S & Q_{12}S & \\ & Q_{21}S & Q_{22}S & \\ \hline & & & \end{array}\right) \left(\begin{array}{c} \dot{h}_{1,1} \\ \dot{h}_{1,2} \\ \dot{h}_{1,3} \\ \dot{h}_{0,2} \\ \hline \pi_1 \\ \pi_2 \\ \hline \dot{x}_- \\ \dot{x}_+ \end{array}\right) = \left(\begin{array}{c} -\sigma Sh_{1,1} \\ -\sigma Sh_{1,2} \\ -\sigma Sh_{1,3} \\ -\sigma Sh_{0,2} \\ \hline 0 \\ 0 \\ \hline +e(x_-) \\ -e(x_+) \end{array}\right) \tag{23}$$

where blank blocks are zero and we call the right side –dF. If we use the notation $\rho = (\rho_{1,1}, \rho_{1,2}, \rho_{1,3}, \rho_{0,2})$ and corresponding for $\tilde{\rho}$ then we have

$$\begin{aligned} \tilde{\rho}\,(\sigma S)\,\rho = &\sum_{ij} \left(\int_{\omega_1} \nabla\varphi_i \cdot \nabla\varphi_j \,\mathrm{d}x \right) (\sigma_1 + \sigma_2) \rho_{1,1}^i \tilde{\rho}_{1,1}^j \\ &+ \sum_{ij} \left(\int_{\omega_3} \nabla\varphi_i \cdot \nabla\varphi_j \,\mathrm{d}x \right) (\sigma_1 + \sigma_2) \rho_{1,3}^i \tilde{\rho}_{1,3}^j \\ &+ \sum_{ij} \left(\int_{\omega_2} \nabla\varphi_i \cdot \nabla\varphi_j \,\mathrm{d}x \right) \big(\sigma_1 \rho_{1,2}^i \tilde{\rho}_{1,2}^j + \sigma_2 (\rho_{1,2}^i + \rho_{0,2}^i)(\tilde{\rho}_{1,2}^j + \tilde{\rho}_{0,2}^j)\big), \end{aligned}$$

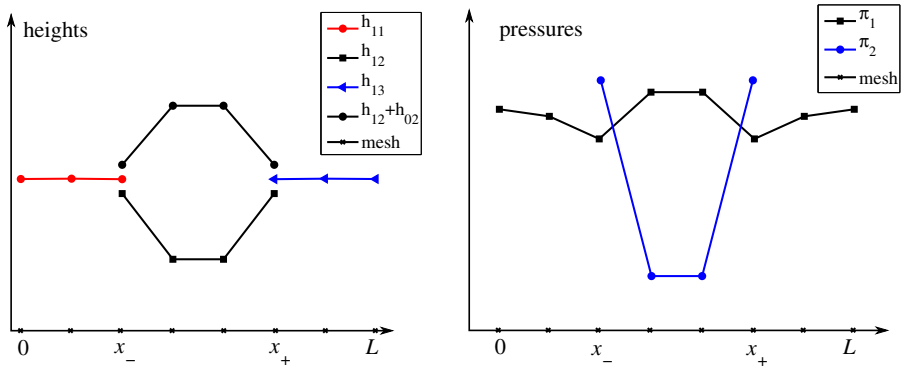

Fig. 3 Sketch of discrete degrees of freedom $\dot{h}_1, \dot{h}$ (*left*) and π_1, π_2 (*right*) on a coarse mesh of 8 vertices

which just represents the part of $\mathrm{diff}\, F(\mathbf{s})[\dot{\mathbf{s}}]$ which is of the form

$$\int_\omega \sigma_1 \nabla\rho_1 \cdot \nabla\tilde{\rho}_1 + \sigma_2(\nabla\rho_1 + \nabla\rho) \cdot (\nabla\tilde{\rho}_1 + \nabla\tilde{\rho})\, \mathrm{d}x$$

in (16). This term appears in the right-hand-side of the problem after replacing h, h_1 by $h + \tau\dot{h}, h_1 + \tau\dot{h}_1$ in $\mathrm{diff}\, F$ to treat the surface energy semi-implicit. To get the corresponding matrices one needs to set either $\rho = (h_{1,1}, h_{1,2}, h_{1,3}, h_{0,2})$ or $\rho = (\dot{h}_{1,1}, \dot{h}_{1,2}, \dot{h}_{1,3}, \dot{h}_{0,2})$. Furthermore we have

$$\tilde{\pi}_k Q_{kl} S \pi_l := \sum_{ij} \left(\int Q_{kl} \nabla\chi_i \cdot \nabla\chi_j \,\mathrm{d}x \right) \pi_l^i \tilde{\pi}_k^j$$

with the noted properties on the domain of definition of π_j. Plugging in the local definition we obtain for instance

$$\tilde{\pi}_1 \left(Q_{11} S\right) \pi_1 = \sum_{ij} \left(\int_\omega \frac{h_1^3}{3\mu} \nabla\chi_i \cdot \nabla\chi_j \mathrm{d}x \right) \pi_1^i \tilde{\pi}_1^j$$

with the basis functions χ_i as introduced before. Note that the matrix above is singular because we added $\dot{x}_\pm$. However, adding the constraints C makes the discrete equation again non-singular and we end-up with a saddle-point problem

$$\begin{pmatrix} D & C^\top \\ C & 0 \end{pmatrix} \begin{pmatrix} \dot{\mathbf{s}} \\ \lambda \end{pmatrix} = \begin{pmatrix} -\mathrm{d}F \\ 0 \end{pmatrix}.$$

Once we have computed $\dot{\mathbf{s}}$ we need to evolve the state $\mathbf{s}(t)$ in X to some approximate but admissible $\mathbf{s}(t+\tau)$ in X. Therefore we propose to decompose $\dot{h}, \dot{h}_1$ using $\dot{x}_\pm$ into partial time-derivatives of $H(t,x) = h(t, \Psi_t(x))$ and $H_1(t,x) = h_1(t, \Psi_t(x))$. Note that the unambiguous Ψ which we introduced in the previous section leads to

$$\dot{\Psi}(x) := \begin{cases} \dot{x}_- \frac{x}{x_-} & x \in \omega_1, \\ \dot{x}_- \left(1 - \frac{x - x_-}{x_+ - x_-}\right) + \dot{x}_+ \left(\frac{x - x_-}{x_+ - x_-}\right) & x \in \omega_2, \\ \dot{x}_+ \left(1 - \frac{L - x}{L - x_+}\right) & x \in \omega_3 \end{cases} \tag{24}$$

with the obvious properties $\dot{\Psi}(0) = \dot{\Psi}(L) = 0, \dot{\Psi}(x_\pm) = \dot{x}_\pm$. The mapping $\Psi(x)$ is equidistant in each ω_i, i.e. $\partial_x \Psi = \text{constant} > 0$ in each ω_i as long as we have $0 < x_-(t) < x_+(t) < L$. One can easily see that

$$\dot{h}(t,x) + \dot{\Psi}(x) \cdot \nabla h(t,x) = \dot{H}(t,x), \quad \dot{h}_1(t,x) + \dot{\Psi}(x) \cdot \nabla h_1(t,x) = \dot{H}_1(t,x)$$

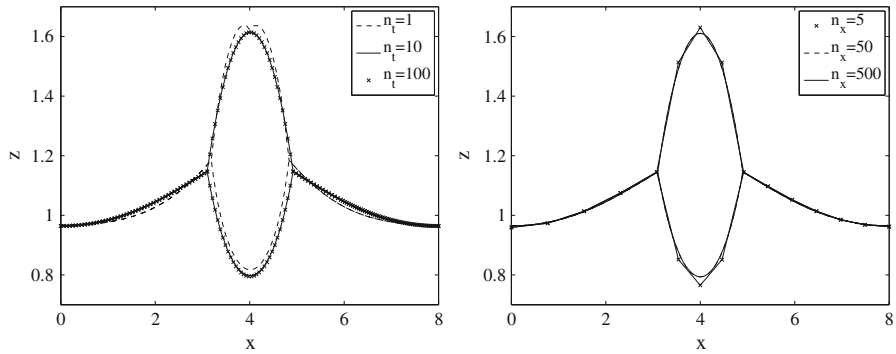

Fig. 4 Convergence of solution (h_1, h, x_-, x_+) at time $t = 1$ depending on number of time-steps n_t (*left*) or spatial discretization n_s (right)

where $\dot{H}$ has zero boundary conditions and $\dot{H}_1$ is continuous at $x_\pm$. In Lagrangian coordinates we can define the updated solution $\mathbf{s} \mapsto \mathbf{s} + \tau\dot{\mathbf{s}} \in X$ by

$$\Psi_{t+\tau}(x) = x + \tau\dot{\Psi}(x), \tag{25a}$$

$$H(t+\tau, x) = h(t, x) + \tau\dot{H}(t, x), \tag{25b}$$

$$H_1(t+\tau, x) = h_1(t, x) + \tau\dot{H}_1(t, x), \tag{25c}$$

so that $h(t+\tau, \Psi_{t+\tau}(x)) := H(t+\tau, x)$ and $h_1(t+\tau, \Psi_{t+\tau}(x)) := H_1(t+\tau, x)$. This is the final step of the numerical algorithm. In practice this update can be achieved by deforming the computational domain $x \to x + \tau\dot{\Psi}$ and updating the corresponding nodal values $h \to h + \tau\dot{H}, h_1 \to h_1 + \tau\dot{H}_1$. Using the map Ψ guarantees that solutions never leave the space of admissible domains. We check the robustness of the algorithm with respect to temporal and spatial discretization for one example.

Example 3.1 Consider the initial data on $\omega = [0, 8]$ with $x_-(0) = 3$ and $x_+(0) = 5$

$$h_1(0, x) = 1, \quad h(0, x) = (1 - |4 - x|)_+$$

with $\tau = 1/n_t$ and $\delta x = |\omega_i|/n_x$ in each ω_i. As parameters for this example we choose

$$\sigma_1 = 1, \quad \sigma_2 = 1, \quad \sigma(x) = \begin{cases} 1 & x \in \omega_2, \\ 0 & \text{else}, \end{cases}$$

The corresponding solution h_1, h are shown in Fig. 4. Each domain is discretized separately, e.g. for ω_1 we have $0 = x_1 < \ldots < x_{N_p} = x_-$ with corresponding standard finite element space. Figure 4 shows the dependence of the solution at $t = 1$. Note that the initial data is not smooth at $x = 4$, still solutions with different n_t roughly agree even for $n_t = 1$. For $n_t \to \infty$ we see typical convergence for a first order method. It seems that at $t \to 0$ there is some loss of volume m_1, m_2 which might be due to the fact the initial data do not satisfy the equilibrium conditions $[[e + b]] = 0, [[c]] = 0$ (Fig. 5). Similarly the method is quite robust when using coarse meshes with as few as $N_p = 5$ points for each interval ω_i. This is particularly interesting for applications of the numerical algorithm in higher dimensions.

In what follows we will also compare the gradient approach with numerical solutions of (1). Corresponding algorithms for thin-film equations with precursor are rather standard and have been discussed throughout the literature. Our implementation uses a fully-implicit time-discretization and second finite-differences in space. Time-step size is adaptively refined using step-size bisection and a Richardson extrapolation.

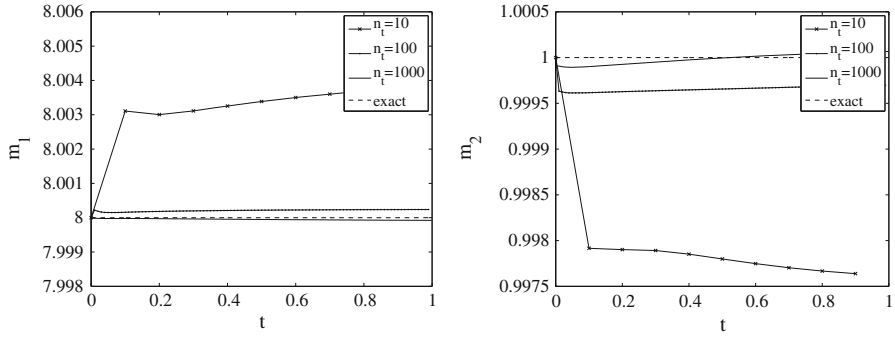

Fig. 5 Convergence mass m_1, m_2 as a function of time depending on time-discretization

4 Validation of gradient model

In this section we are going to compare the numerical solutions of the gradient formulation with other solutions of thin-film bilayer systems. First we compare solutions to solutions of a bilayer systems with precursor and then we compare with an asymptotically exact source-type solutions for a spreading droplet on a liquid substrate with $\sigma(x) \equiv 0$.

4.1 Comparison with precursor model

Consider the precursor energy

$$F_*(h_1, h) = \int_\omega \frac{\sigma_1}{2}|\nabla h_1|^2 + \frac{\sigma_2}{2}|\nabla h_1 + h|^2 + \sigma V_*(h)\,\mathrm{d}x$$

corresponding to the model (1), where h_* is a small positive parameter controlling the minimum thickness of h. Using $\pi_1 = \delta F_*/\delta h_1$ and $\pi_2 = \delta F_*/\delta h$ gives the formulation (1) from Sect. 1. Stationary solutions of (1) are known to minimize F_* subject to the constraint that we keep the mass fixed, i.e.,

$$\{h_1^*, h^*\} = \operatorname*{argmin}_{\mathcal{X}} F_*,$$

where $\mathcal{X} = \{(h_1, h) \in H^1(\omega)^2, m_1 = M_1, m_2 = M_2, h_1 > 0, h \geq 0\}$. Limiting properties of such a sequence of minimizers $\{h_1^*, h^*\}_{h_*}$ can be shown in the framework of Γ-convergence. In a previous paper we showed that

$$\Gamma\text{-}\lim_{h_*\to 0} F_* = \int_\omega \frac{\sigma_1}{2}|\nabla h_1|^2 + \frac{\sigma_2}{2}|\nabla h_1 + h|^2 + \sigma\chi\{h > 0\}\,\mathrm{d}x \equiv F,$$

i.e., roughly speaking we have that $\{h_1^*, h^*\}_{h_*}$ (weakly) converge as $h_* \to 0$ and the limit minimizes F [22]. Using an rearrangement argument we rigorously showed that minimizers of F are liquid lenses

$$h_1(x) = \hat{H}_1 - \rho(\hat{H}_0 - |x - x_0|^2)_+, \quad h(x) = \kappa(\hat{H}_0 - |x - x_0|^2)_+$$

with for $\hat{H}_0, \hat{H}_1, \rho, \kappa \in \mathbb{R}^+$ determined by the constraints $[[e + b]] = 0, [[c]] = 0, m_1 = M_1, m_2 = M_2$ and $x_0 \in \omega \subset \mathbb{R}^{d-1}$ arbitrary. To keep the proof this general we had to work with balls $\omega = B_r$ and then we need to choose x_0 so that $\{h > 0\} \subset \omega$. A typical stationary solution from the precursor model and the gradient model are shown in Fig. 6.

We study instationary solutions of Example 3.1 in order to provide a comparison of the sharp triple-junction model with those of the precursor model. As initial data for the precursor model we used $h_1^*(0, x) = h_1(0, x) - h_*/2$ and $h^*(0, x) = h(0, x) + h_*/2$ with $h_* = 1/512$ and $h_* = 1/16$. In the implementation of the sharp-interface model we start with time-step sizes $\tau = 10^{-6}$ and perform $n_t = 300$ iteration. Afterwards we successively increase

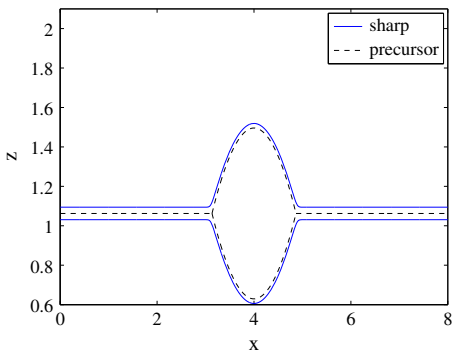

Fig. 6 Stationary solutions of sharp triple-junction transient solutions from example 3.1 (*solid lines*) with $h_1^*(0,x) = h_1 - h_*/2$, $h^*(0,x) = h + h_*/2$ as initial data for the precursor problem and $h_* = 1/16$ (*dashed lines*)

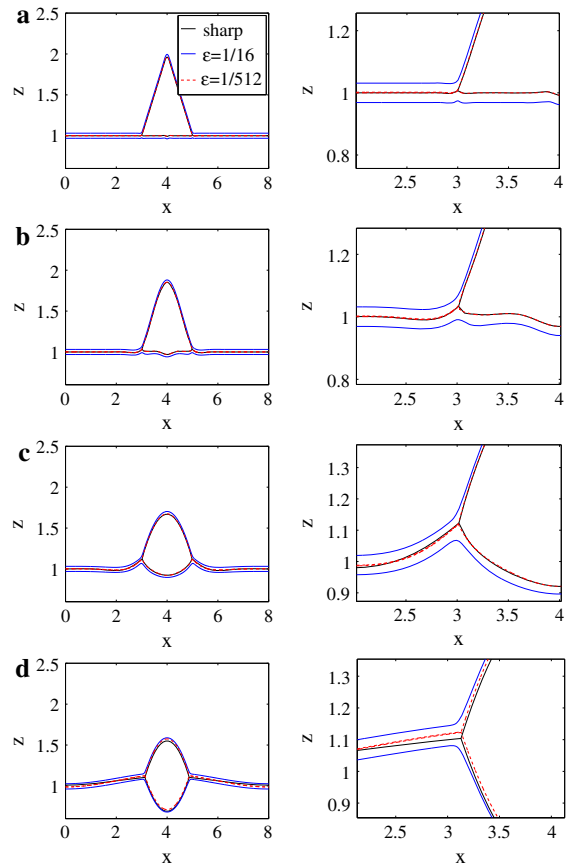

Fig. 7 Evolution of gradient model and precursor model at different times **(a)** $t = 3 \cdot 10^{-6}$, **(b)** $t = 10^{-3}$, **(c)** $t = 3 \cdot 10^{-2}$, **(d)** $t = 4$, from top to bottom. The *upper* plot shows the overall solution, whereas the *lower* plot focuses on the solution near the contact line. For $t < 10^{-2}$ solutions of both models are nearly indistinguishable

$\tau \to 10\tau$ and repeat that procedure until we are sufficiently close to the stationary states. Corresponding solutions of both models and at different times are shown in Fig. 7. The left panel shows the solution and the right panel shows a close-up of the triple-junction. For $t \ll 1$ the solutions of both models shown in Fig. 7 are very close, difference are only visible on the scale 10^{-3}. At larger times numerical solutions deviate, where the general structure of the solution seems to remain the same but the gradient formulation is ahead in time. For example it reaches the stationary state at $t \sim 10$ and h_1 is almost flat in the region $\omega_1 \cup \omega_3$, whereas h_1^* of the precursor model is still curvy. Looking at the excellent agreement at early times where both methods use small time-steps we propose that this difference is due to the implicit time-step overdamping the evolution in the precursor model. To overcome this problem a different time-integration scheme should be used. As expected, stationary solutions show an excellent agreement and differences are mainly due to mass differences due to the definition of the precursor. In Fig. 6 a stationary solution with a rather big precursor $\varepsilon = 1/16$ is compared with a stationary solution of the gradient formulation.

4.2 Source-type solutions for $\sigma = 0$

In order to validate the gradient model and to show its capabilities we will derive source-type solutions of (2) in this section and compare with numerical solutions. As a class of special solutions featuring contact-line motion

source-type solutions on solid substrate have gotten some attention in the past. On a solid substrate it is known that the exponent in the mobility matrix $q(h) = h^\nu$ in the thin-film equation

$$\partial_t h - \nabla \cdot (q \nabla \pi) = 0, \qquad \pi = -\Delta h$$

determines properties of solutions. Bernis et al. [23] proved that for each $0 < \nu < 3$ there is a unique even solutions and it has compact support. For $\nu \geq 3$ they prove nonexistence of nontrivial solutions. The structure of solutions near the triple-junction (solid/liquid/air) was worked out by Giacomelli et al. [24]. In the context of bilayer flows we seek source-type solution $h_1(t, x)$, $h(t, x)$ of the special form

$$h_1(t, x) = 1 - H(\eta)t^{-\alpha}, \qquad h(t, x) = G(\eta)t^{-\alpha},$$

where $\eta = xt^{-\alpha}$ and $\alpha > 0$. The approximation we are going to make assume $t \to \infty$ and thereby $Ht^{-\alpha} \ll 1$. Plugging this ansatz into (2) we obtain

$$\alpha t^{-\alpha-1}(\eta H)' = t^{-2\alpha}\left(Q_{11}\pi_1' + Q_{12}\pi_2'\right)', \tag{26}$$

$$-\alpha t^{-\alpha-1}(\eta G)' = t^{-2\alpha}\left(Q_{21}\pi_1' + Q_{22}\pi_2'\right)', \tag{27}$$

where $(\cdot)' = \partial_\eta(\cdot)$. The mobility matrix reads

$$Q = \frac{1}{\mu}\begin{pmatrix} \frac{1}{3}(1 - H(\eta)t^{-\alpha})^3 & \frac{1}{2}(1 - H(\eta)t^{-\alpha})^2 G(\eta)t^{-\alpha} \\ \frac{1}{2}(1 - H(\eta)t^{-\alpha})^2 G(\eta)t^{-\alpha} & \frac{\mu}{3}(G(\eta)t^{-\alpha})^3 + (1 - H(\eta)t^{-\alpha})(G(\eta)t^{-\alpha})^2 \end{pmatrix}$$

and the generalized pressures are

$$\pi_1 = \big((\sigma_1 + \sigma_2)H'' - \sigma_2 G''\big)t^{-3\alpha}, \quad \pi_2 = \sigma_2\big(H'' - G''\big)t^{-3\alpha}. \tag{28}$$

Now, we balance our equations such that the leading order of mobility matrix Q does not become singular. To ensure this we let α fulfill $-\alpha - 1 = -7\alpha$, that is $\alpha = 1/6$. Asymptotic expansions of H and G with respect to $t^{-\alpha}$, i.e. $H = H_0 + t^{-\alpha}H_1 + o(t^{-\alpha})$, $G = G_0 + t^{-\alpha}G_1 + o(t^{-\alpha})$, give the leading order equation

$$0 = \big((\sigma_1 + \sigma_2)H_0'' - \sigma_2 G_0''\big)''. \tag{29}$$

Since for large times we expect h_1 to become flat on the $\omega_1 \cup \omega_3$ we get

$$H_0 = \frac{\sigma_2}{\sigma_1 + \sigma_2} G_0. \tag{30}$$

The function G_0 will be derived from the next order

$$0 = \left(\frac{1}{3\mu}\big((\sigma_1 + \sigma_2)H_1'' - \sigma_2 G_1''\big)' + \frac{\sigma_2}{2\mu} G_0\big(H_0'' - G_0''\big)'\right)', \tag{31}$$

$$-\frac{1}{6}(\eta G_0)' = \left(\frac{1}{2\mu} G_0\big((\sigma_1 + \sigma_2)H_1'' - \sigma_2 G_1''\big)' + \frac{\sigma_2}{\mu} G_0^2\big(H_0'' - G_0''\big)'\right)'. \tag{32}$$

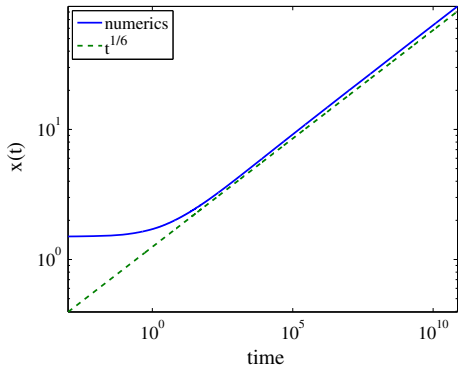

Fig. 8 Half-width of the spreading droplet $(x_+ - x_-)/2$ as a function of time shows the predicted $t^{1/6}$ power law

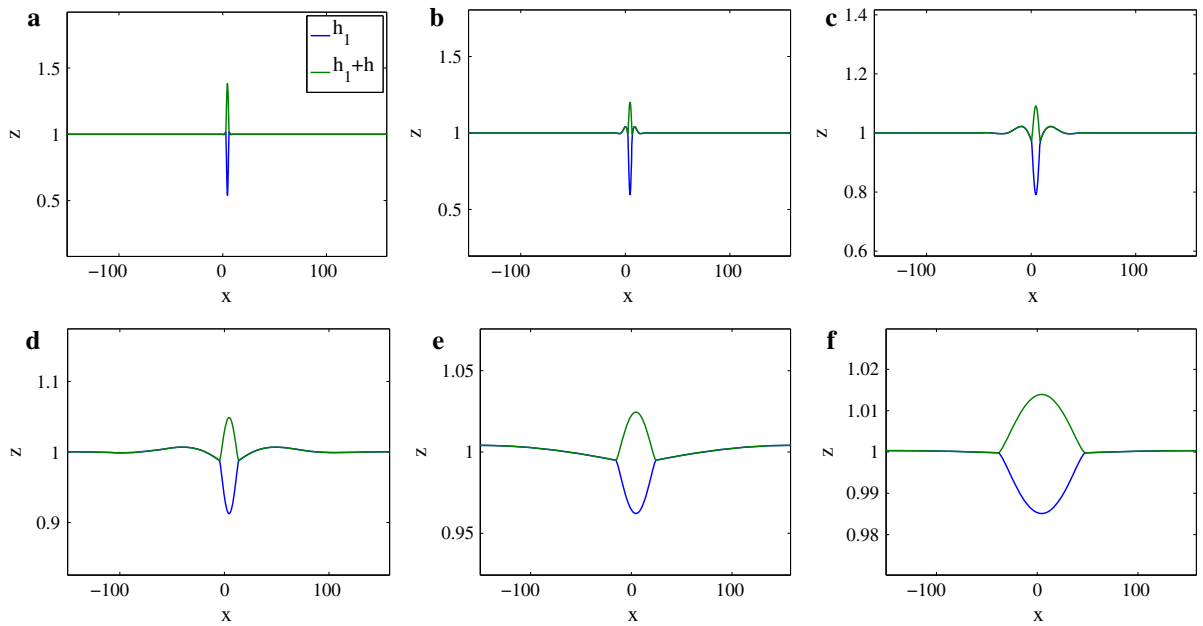

Fig. 9 Spreading of droplet converging to a source-type solution. Note that the scales change as $t \to \infty$. The total volume of both liquids is conserved with a relative precision $(m_i(0) - m_i(t))/m_i(0) \sim 10^{-3}$ for $0 < t < 10^{10}$. The times are (**a**)–(**f**) $t = 10^{-1}, 10^{1}, \ldots, 10^{9}$ respectively

Putting the last three equations together we get

$$(\eta G_0)' = \left(\frac{3\sigma_1\sigma_2}{2\mu(\sigma_1+\sigma_2)} G_0^2 G_0''' \right)' . \tag{33}$$

This is the equation for source-type solutions with $\alpha = 2$. The difference to thin-films on a solid substrate is that this solution is only asymptotically valid, when $Ht^{-\alpha} \ll 1$. For short times higher order corrections $G_1, G_2, \ldots$ would be needed to improve the accuracy of solutions. In Fig. 8 we show half-width of the spreading droplet $(x_+ - x_-)/2$ for a solution with initial data $h = (1-x)_+$ and $h_1 = 1 - h/2$ in $\omega = (-150, 150)$. The time-steps are increased according to the power-law to avoid contact line motion to become too fast or too slow. The solution at different times is shown in Fig. 9. Note that even though the $t^{1/6}$ power-law of Fig. 8 sets in already at $t \sim 10^2$, the solutions resemble the source-type solution with $h_1 \equiv 1$ for $x > x_+$ or $x < x_-$ only for $t \gtrapprox 10^8$.

As one can clearly see that the contact line nicely resembles the expected power-law for sufficiently large times. What is known about the solution G_0 is that

$$G_0(\eta) = A(\eta \pm \eta_0)^{3/2}(1 + o(\eta \pm \eta_0)$$

as $\eta \to \pm\eta_0$ where η_0 is the rescaled position of the triple-junction.

Since the equation is scaling-invariant we can set $\eta_0 = 1$. The function G_0 can be easily determined by a boundary value problem which we solve using a Runge-Kutta ODE integrator of 5th order combined with a shooting method. The comparison of both rescaled profiles G_0 and the rescaled profile from the gradient model are shown in Fig. 10. The remaining differences are probably due to the fact that with $h \sim 10^{-2}$ the solution still requires higher order corrections and the mesh for solving the PDE was quite coarse. Note that the PDE solution shows the above-mentioned behavior $(\eta \pm \eta_0)^{3/2}$. We are unable to compare higher order corrections $o(\eta \pm \eta_0)$ also because the used mesh was rather coarse, but we showed the capability of the gradient approach to capture the motion of the triple-junction for zero contact angle and also to capture the corresponding singularity $G_0(\eta) \sim (\eta \pm \eta_0)^{3/2}$. This is of course a necessary prerequisite for a sharp-interface gradient model.

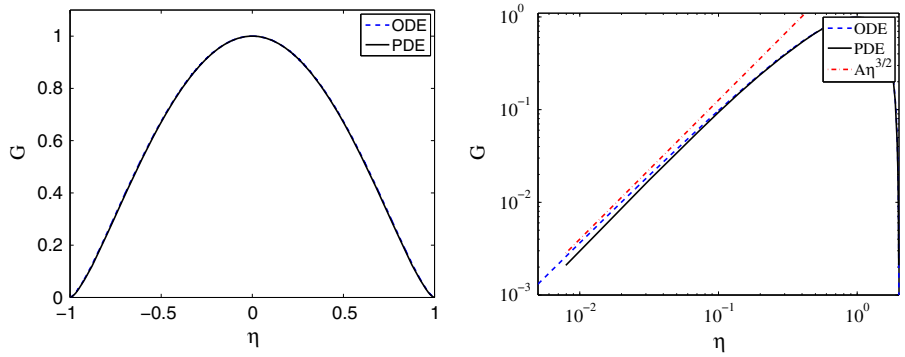

Fig. 10 (*left*) Comparison of PDE solution with ODE solution and (*right*) comparison near $\eta' = \eta + 1 \sim 0$

5 Conclusion

Starting from gradient flow formulation of a two-phase Stokes flow we motivated a corresponding gradient structure for a thin-film bilayer model. In both models the triple-junction is treated explicitly. Boundary conditions at the triple-junction followed either from the definition of the space of states X or from the gradient of the surface energy. We identified the resulting gradient with the well known model for sharp-interface bilayer flow of Kriegsmann [7].

The gradient formulation admits a natural discretization in a finite element framework, where constraints of the solution space are enforced by Lagrange multipliers on a discrete level. We showed that the algorithm is robust in terms of the solution quality for large time-steps and on coarse grids and can be extended to 3D. We compared numerical solutions of the sharp-interface model with those of the precursor model and found excellent agreement for short and moderate times. However, for large times solutions of the precursor model seemed to be overdamped. Furthermore we confirmed convergence of numerical solutions of the gradient model to asymptotic source-type solutions for quadratic mobility and find excellent agreement in terms of the power-law and the shape of the source-type solution for $t \to \infty$. All this leads us to believe that the sharp-interface gradient formulation is a useful technique to model spreading and dewetting of bilayer flows and is also a natural structure for numerical algorithms.

Acknowledgments SJ and DP thank the German Research Foundation DFG for financial support through the project *Structure formation in thin liquid–liquid films* in the SPP 1506 and DFG Research Center MATHEON through the project C10. The work of GK was supported by the postdoctoral scholarship at the *Max-Planck-Institute for Mathematics in the Sciences* in Leipzig. We also thank Maciek Korzec (Technical University Berlin) for useful discussions.

References

1. Oron A, Davis SH, Bankoff SG (1997) Long-scale evolution of thin liquid films. Rev Mod Phys 69(3):931
2. Huh C, Scriven LE (1971) Hydrodynamic model of steady movement of a solid/liquid/fluid contact line. J Colloid Interface Sci 35(1):85–101
3. Hervet H, de Gennes PG (1984) The dynamics of wetting: precursor films in the wetting of dry solids. Comptes Rendus de l'Académie des Sci 299:499–503
4. de Gennes PG, Brochard-Wyart F, Quéré D (2004) Capillarity and wetting phenomena: drops, bubbles, pearls, waves. Springer, Berlin
5. Joanny JF (1987) Wetting of a liquid substrate. Physicochem Hydrodyn 9(1–2):183–196
6. Brochard-Wyart F, Martin P, Redon C (1993) Liquid/liquid dewetting. Langmuir 9(12):3682–3690
7. Kriegsmann JJ, Miksis MJ (2003) Steady motion of a drop along a liquid interface. SIAM J Appl Math 64(1):18–40
8. Pototsky A, Bestehorn M, Merkt D, Thiele U (2004) Alternative pathways of dewetting for a thin liquid two-layer film. Phys Rev E 70(2):025201
9. Craster RV, Matar OK (2006) On the dynamics of liquid lenses. J Colloid Interface Sci 303(2):503–516
10. Karapetsas G, Craster RV, Matar OK (2011) Surfactant-driven dynamics of liquid lenses. Phys Fluids 23(12):122106–122106
11. Danov KD, Paunov VN, Alleborn N, Raszillier H, Durst F (1998) Stability of evaporating two-layered liquid film in the presence of surfactant. Chem Eng Sci 53(15):2809–2822

12. Kriegsmann JJ (1999) Spreading on a liquid film. PhD thesis, Northwestern University
13. Jachalski S, Kitavtsev G, Taranets R (2014) Weak solutions to lubrication systems describing the evolution of bilayer thin films. Commun Math Sci 12(3):527–544
14. Escher J, Matioc BV (2014) Non-negative global weak solutions for a degenerated parabolic system approximating the two-phase Stokes problem. J Differ Equ 256(8):2659–2676
15. Merkt D, Pototsky A, Bestehorn M, Thiele U (2005) Long-wave theory of bounded two-layer films with a free liquid-liquid interface: short-and long-time evolution. Phys Fluids 17:064104
16. Otto F (2001) The geomety of dissipative evolution equations: the porous medium equation. Commun Partial Differ Equ 26(1–2):101–174
17. Rumpf M, Vantzos O (2013) Numerical gradient flow discretization of viscous thin films on curved geometries. Math Models Methods Appl Sci 23(05):917–947
18. von Helmholtz H (1868) Theorie der stationären Ströme in reibenden Flüssigkeiten. Verh Naturh-Med Ver Heidelb 11:223
19. Rayleigh JWS (1913) On the motion of a viscous fluid. Philos Mag 6(26):621–628
20. Neumann FE (1894) Vorlesung über die Theorie der Capillarität. BG Teubner, Leipzig, pp 113–116
21. Otto F (1998) Lubrication approximation with prescribed nonzero contact angle. Commun Partial Differ Equ 23(11–12):2077–2164
22. Jachalski S, Huth R, Kitavtsev G, Peschka D, Wagner B (2013) Stationary solutions of liquid two-layer thin-film models. SIAM J Appl Math 73(3):1183–1202
23. Bernis F, Peletier LA, Williams SM (1992) Source type solutions of a fourth order nonlinear degenerate parabolic equation. Nonlinear Anal Theory Methods Appl 18(3):217–234
24. Giacomelli L, Gnann MV, Otto F (2013) Regularity of source-type solutions to the thin-film equation with zero contact angle and mobility exponent between 3/2 and 3. Eur J Appl Math 24:735–760